Springer

Acta Mechanica Sinica

CrossMark click for updates

• RESEARCH PAPER •

Acta Mech. Sin., Vol. 39, 723016 (2023)
https://doi.org/10.1007/s10409-023-23016-x

Glide-reflection symmetric phononic crystal interface: variation on a theme

Vincent Laude[1*], Julio Andrés Iglesias Martínez[1], Nicolas Laforge[1], Muamer Kadic[1], and Emil Prodan[2]

[1] *Université de Franche-Comté, CNRS, institut FEMTO-ST, Besançon, France;*
[2] *Department of Physics, Yeshiva University, New York, USA*

Received January 12, 2023; accepted March 17, 2023; published online May 6, 2023

Nodal points can be artificially synthesized using glide-reflection symmetries at crystal interfaces. This property was first demonstrated for a square-lattice phononic crystal at the X point of the first Brillouin zone (wavenumber $k = \pm\pi/a$ with a the lattice constant), for a half-lattice-constant glide. Here we show that the nodal point can be moved to the Γ point ($k = 0$) considering quarter-lattice-constant glide-reflection symmetry. Applying a continuous grading along the x-axis is further shown to leave the band structure mostly unaffected. In particular, the topological interface waves survive in the case that glide-reflection symmetry is only locally valid around the graded interface. As a result, the glide dislocation can be compensated for over a distance of a few crystal rows, to recover an apparently periodic crystal.

Phononic crystal, Glide-reflection symmetry, Phononic crystal waveguide

Citation: V. Laude, J. A. I. Martínez, N. Laforge, M. Kadic, and E. Prodan, Glide-reflection symmetric phononic crystal interface: variation on a theme, Acta Mech. Sin. **39**, 723016 (2023), https://doi.org/10.1007/s10409-023-23016-x

1. Introduction

Topological metamaterials have recently arisen as novel avenues for tailoring the properties of artificial crystals, including photonic and phononic crystals [1-7]. Mathematically, the topological properties that characterize different phases of a crystal are derived from Bloch waves, or eigenvectors, including their Berry phases [8, 9]. The Berry phase, a geometrical phase defined for periodic systems, complements the usual phase of the eigenvalue, that depends on the Bloch wavevector k defined in the first Brillouin zone. Edge waves can be obtained along domain walls separating two topologically different phases of the same crystal [10-15].

In this paper, we consider the case of time-reflection symmetric (TRS) waveguides created by a glide dislocation in a two-dimensional (2D) phononic crystal [16]. Because of the dislocations, these systems have only one periodicity (1D) left, but they still inherit the phononic band properties of the parent 2D crystal, hence constituting the bulk crystal from which the boundary, or interface, is created. The space group of a 1D periodic structure is also known as a frieze group. There are a total of 7 frieze groups, among which only the two groups p11g and p2mg possess a half-lattice glide-reflection symmetry (GRS). Recently, it has been shown that crystal interfaces belonging to these two frieze groups support a pair of non-interacting, or backscattering-free, guided waves with a smooth dispersion covering a large part of the 2D phononic band gap [16]. The band structure topology of those crystal interfaces is protected by the GRS. Glide-reflection symmetry belongs to nonsymmorphic symmetries, i.e., symmetries that do not leave a fixed point invariant inside the unit cell. Band inversion is obtained at the X point of the first Brillouin zone, i.e., at its edges. The crossing-point of the two guided bands is one example of a nodal point of

*Corresponding author. E-mail address: vincent.laude@femto-st.fr (Vincent Laude)
Executive Editor: G. L. Huang

the 1D band structure, similar to Dirac points in 2D and two-dimensional (3D) crystals.

In this paper, we further extend the theory of the glide-reflection symmetric phononic crystal interface in two different directions. First, we show that the nodal point can be moved from the X point to the Γ point of the first Brillouin zone, by introducing a quarter-lattice-constant glide-reflection symmetry, when the 2D crystal unit cell is extended by a factor two along the interface direction (the extended lattice constant $a_x = 2a$, with a the original lattice constant). The extended unit cell contains two different inclusions per unit cell, separated by a, such that taken separately they both lead to a similar complete phononic band gap range. Moving the nodal point to the Γ point, that is to a zero or integer value of the reciprocal lattice constant, may find applications for normal incidence excitation of the 1D waveguide. Second, we discuss the locality of the constraint of GRS of the crystal interface and show that it can be deformed continuously to compensate for the glide dislocation away from the interface, while keeping in an approximate and local sense the topological properties of a buried GRS interface.

2. Quarter-lattice-constant glide-reflection symmetry

Let us first recall a few facts regarding the half-lattice-constant glide-reflection symmetric crystal interface. Figure 1a depicts the spatial arrangement of the crystal interface. The glide-reflection symmetry acts on coordinates as $(x, y) \to (x + a/2, -y)$. Applied twice, it results in a translation of the crystal structure by exactly one lattice constant a, or

$$G_{a/2} \circ G_{a/2} = T_a \tag{1}$$

in terms of symmetry operators. The latter property is the origin of the degeneracy at the X point of the first Brillouin zone ($k = \pi/a$). Indeed, in reciprocal space $G_{a/2}(k)^2 = \exp(\mathrm{i}ka)$ with k the Bloch wavevector, so that

$$G_{a/2}(\pi/a)^2 = -1. \tag{2}$$

Hence the eigenvalues of the GRS operator are $\pm\mathrm{i}$ with complex-conjugated eigenvectors u and u^*. Since the GRS operator and the (real-valued) dynamic operator for elastodynamics commute, they share common eigenvectors and we conclude that bands are degenerate by pairs at the X point.

Let us now elaborate the quarter-lattice-constant glide-reflection symmetric crystal interface from the previous configuration. Figure 1b depicts a unit-cell extended by a factor two in the x-direction, composed of the previous inclusion (labelled A) and of a slightly different inclusion labelled A′. We assume that the complete phononic band gap is almost preserved when changing the inclusion from A to A′, in an adiabatic sense. As an example, we consider in Fig. 2a the square lattice crystal of steel rods in water, with diameter $d = 0.9a$ for inclusion A and $d' = 0.8a$ for inclusion A′. Inclusion A is exactly the same as in Ref. [16] whereas inclusion A′ is slightly reduced while essentially preserving the band gap width. When combined together in the double unit cell without any glide, inclusions A and A′ lead to a fully opened complete band gap. When the glide parameter is set to $g = a_x/2$, as shown in Fig. 2b, degeneracy of all bands by pairs at the point X is obtained. Since the number of bands has been doubled, however, there are no really practically usable guided waves appearing inside the band gap. When the glide parameter is set to $g = a_x/4$, a quarter of the new lattice constant, nodal points appear at the Γ point of the Brillouin zone, as Fig. 2c shows. In particular, there is a pair of non-interacting guided waves, whose bands cross near the

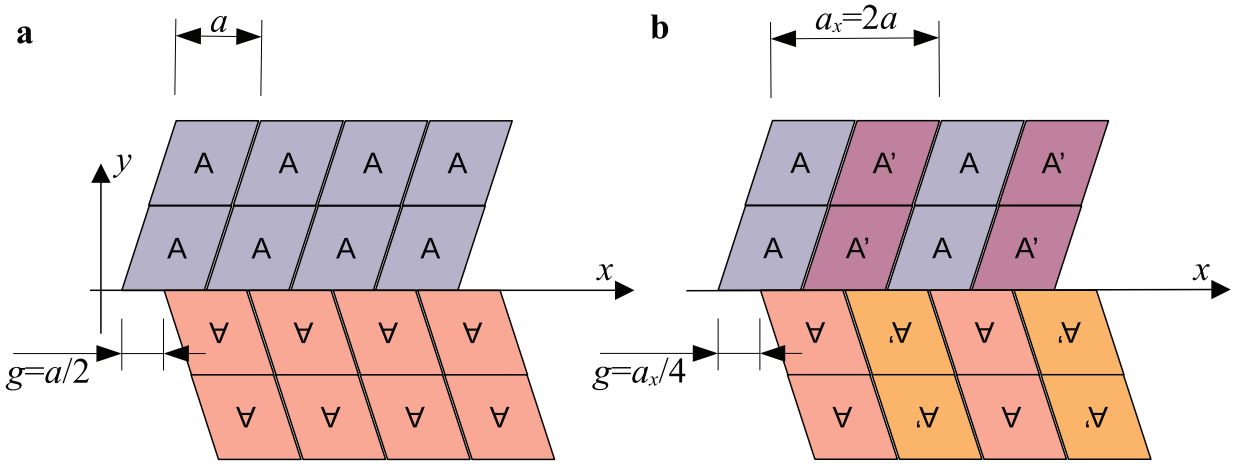

Figure 1 Schematic representation of GRS crystal interfaces, with a the lattice constant of the initial 2D crystal and g the glide parameter. **a** half-lattice-constant GRS interface and **b** quarter-lattice-constant GRS interface.

center of the complete band gap. In the latter case, the glide operator must be applied four times to result in a translation of the crystal structure by exactly one lattice constant a_x. In reciprocal space, we then have $G_{a_x/4}(k)^4 = \exp(\mathrm{i}ka_x)$. At the Γ point,

$$G_{a_x/4}(0)^4 = 1, \tag{3}$$

so that there are four eigenvalues, $(\pm 1, \pm \mathrm{i})$. The first two eigenvalues do not lead to a degeneracy, so that half of the bands remain non degenerate in Fig. 2c. The last two eigenvalues, however, again lead to a degeneracy by pairs of bands (symmetric/antisymmetric with respect to the GRS). Degeneracy occurs for $k = 0$ or an integer number of reciprocal lattice constants, hence at the Γ point. This pair of guided interface waves is perfectly usable for single-mode guidance. The corresponding modal shapes are shown for the pressure part of the Bloch waves in Fig. 3. In particular, the lower guided band (A label) holds a GSR anti-symmetric guided wave, whereas the upper guided band (B label) holds a GSR symmetric guided wave. The band with label C is non degenerate and almost flat.

As a note, the quarter-lattice-constant GRS identifies with the half-lattice-constant GRS when $d = d'$, which is also consistent with the fact that $a_x/4 = a/2$. Hence, the topological invariant that is behind the appearance of guided waves along the interface is the same, the π jump of the 2D Zak phase [17, 18] of Bloch bands of the initial 2D crystal. In practice, moving the nodal point from the X to the Γ point of the first Brillouin zone could be useful for the external excitation of the crystal interface under normal incidence.

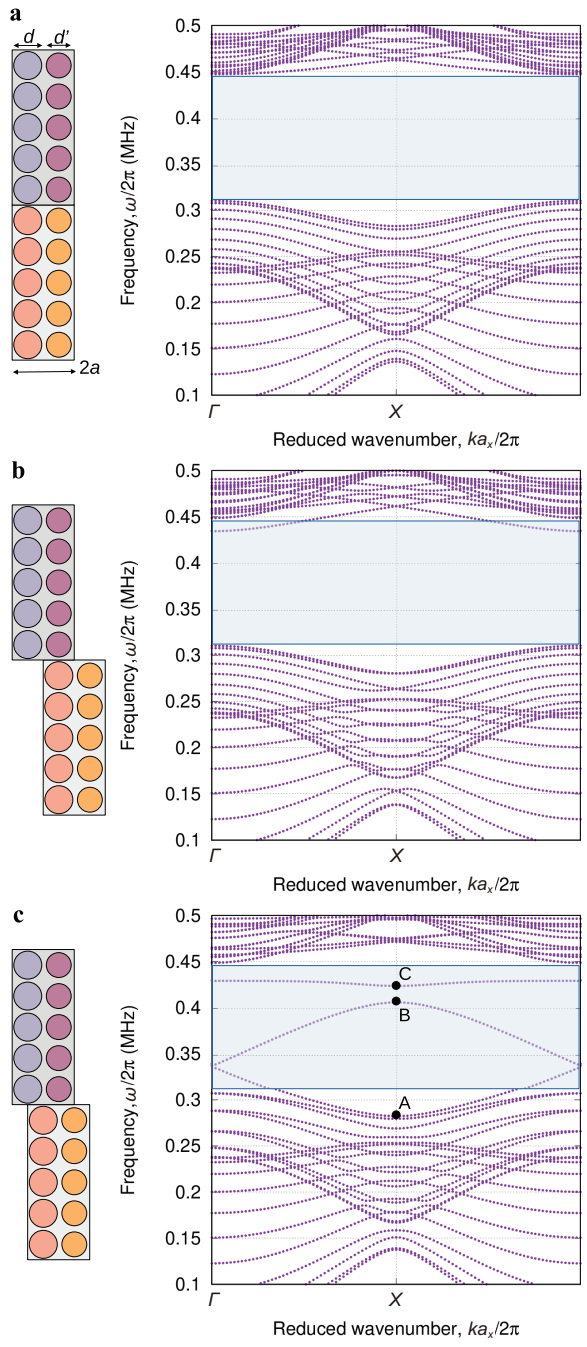

Figure 2 Glide-reflection symmetric crystal interface created by extending the unit-cell of a square-lattice phononic crystal of steel rods in water. The unit-cell extended along the x-axis contains an inclusion with diameter $d = 0.9a$ and an inclusion with diameter $d' = 0.8a$. The rectangular extended unit-cell has horizontal length $a_x = 2a$. Periodic boundary conditions relate the left and right sides of the unit-cell. There are 10 steel rods along the y direction. **a** When the glide parameter $g = 0$, a large complete phononic band gap extends essentially over the phononic band gap with a single inclusion. **b** When $g = a_x/2$, all bands are degenerate by pair at the X point of the first Brillouin zone. **c** When $g = a_x/4$, half the bands are degenerate by pair at the Γ point whereas the other half are not.

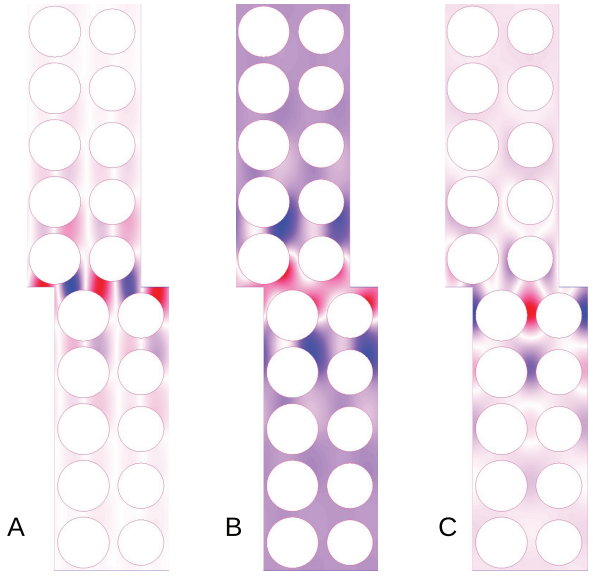

Figure 3 Real part of the normalized modal shapes for pressure, for the guided Bloch waves marked A, B, and C in Fig. 2c. The colorbar varies from blue (minimum) to red (maximum).

3. Graded GRS crystal

Symmetry protection by the glide-reflection ensures that the band structure is not strongly affected under a limited continuous deformation of the crystal lattice. In Ref. [16] the continuous transition from the square lattice to the oblique lattice was considered as an illustration of this principle, that goes far beyond resistance to crystal disorder. Of course, the continuous deformation should also preserve mostly the complete phononic band gap, for the spectral range of appearance of the guided interface waves to remain in operation.

Here we consider a continuous deformation of the crystal lattice that is added to the glide dislocation of the interface. Specifically, the vertical sides of the supercell of the crystal interface are transformed from $x_m = ma$ to $x_m = ma + h(y)$ for $y > 0$. In the example considered in Fig. 4, function $h(y) = (g/2)\sin^2[\pi y/(2na)]$ with n the number of crystal rows. In order to respect glide-reflection symmetry, one must have $h(-y) = h(y)$. As a result, the glide dislocation is conserved vertically and the bottom and top sides of the supercell are glided by g. As Fig. 4a illustrates, the band structure of the graded GRS crystal interface is very similar to the original one (i.e., compared to Fig. 2b of Ref. [16]). The modal shapes for the guided Bloch waves are further similar to the ungraded case and are not reproduced here.

Compensating for the glide away from the interface, for instance to recover the original, perfectly periodic 2D crystal, requires antisymmetry of the grading function: $g(-y) = -g(y)$. Indeed, for the example considered in this section, we would have $h(-na/2) = -g/2$ and $h(na/2) = +g/2$, so that the horizontal displacements at bottom and top cancel the glide g. This choice, however, breaks glide-reflection symmetry and should lead to the opening of a band gap for guided waves at the X point of the first Brillouin zone. If the slope of function $h(y)$ is vertical along the interface, i.e., if $\frac{dh}{dy}(0) = 0$, then the gap opening can be minimized, because the interface still appears locally glide-reflection symetric, at least for the first few crystal rows around the interface. In the example of Fig. 4b, this property is verified.

Transmission through the finite graded crystal interface was investigated numerically, as summarized in Fig. 5, to check the above property. The entrance of the waveguide is excited from a curved focusing line source, with prescribed acceleration. The pressure at the exit of the waveguide is collected on a similar, symmetrically placed curved line. A radiation boundary condition is imposed on the outer circular boundary enclosing the computation domain. The frequency response function (FRF) is defined as the ratio of collected to emitted pressure; it includes the effect of reflections at the entrance and the exit of the waveguide, and the direct emission of pressure waves to the left of the line source. Notably,

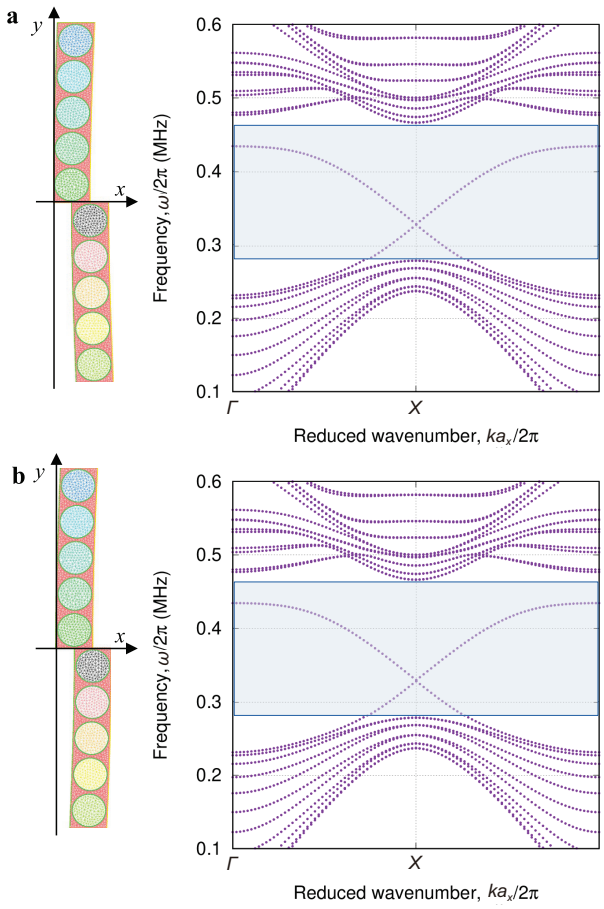

Figure 4 The phononic crystal interface is continuously graded along the x-direction, in addition to the half-lattice constant dislocation. Periodic boundary conditions relate the left and right sides of the unit-cell. There are 10 steel rods along the y direction. **a** In presence of the strict glide-reflection symmetry, the band structure for the crystal interface is almost unchanged compared to the non-graded crystal. **b** With a combination of inversion symmetry and half-lattice glide, but a vertical grading slope on the interface, local glide-reflection symmetry applies only to the first few crystal rows but the band structure is almost unaffected. The pair of guided interface waves almost do not interfere at the X point of the first Brillouin zone.

it is found that the responses for strict and local glide-reflection symmetry are almost coincident, except for the spectral range around the X-point crossing of interface waves, and that no wave cancellations occur as a function of frequency. As a note, the non-zero reflection coefficients at the entrance and the exit of the waveguide lead to spectral interference and cause the appearance of a channeled spectrum [19].

4. Conclusion

As noted in Ref. [16] the glide-reflection symmetric crystal waveguide offers wide bandwidth, single mode operation, and symmetry-protected backscattering immunity. In this

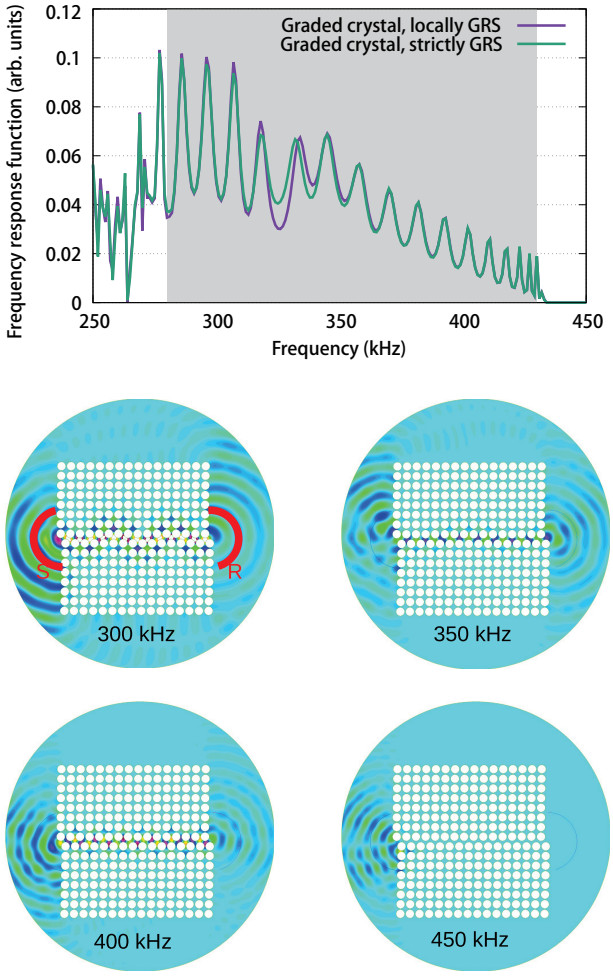

Figure 5 Transmission through a phononic crystal interface is continuously graded along the x-direction, in addition to the half-lattice constant dislocation. The two cases of strict and local glide-reflection symmetry are considered. Pressure waves in water are excited and detected along circles of arc centered on the entrance and on the exit of the interface (S: source; R: receiver). Continuous transmission is observed in either case. Pressure fields are shown for four particular frequencies, in the local GRS case.

paper, we have further extended the concept in two directions. First, we have shown that the nodal point created by GRS can be moved from the X to the Γ point of the first Brillouin zone considering quarter-lattice-constant glide-reflection symmetry for a unit-cell twice extended in the x-direction and containing two slightly different inclusions. Second, applying a continuous variation along the x-axis of the unit cell boundaries, it is further observed that the band structure remains mostly unafected. In particular, interface waves survive in the case that glide-reflection symmetry is only valid locally around the graded interface. As a result, the glide can be compensated for a few crystal rows away from the dislocation.

Author contributions *Vincent Laude, Muamer Kadic and Emil Prodan designed the research and methodology. Julio Andrés Iglesias Martínez and Nicolas Laforge designed computer programs. All authors analyzed the results. Vincent Laude wrote the first draft of the manuscript. All authors revised and edited the final version.*

Acknowledgements *This work was supported by the EIPHI Graduate School (Grant No. ANR-17-EURE-0002) and the U.S. National Science Foundation (Grant Nos. DMR-1823800, CMMI-2131760 and CMMI-1930873). Finite element programming was performed using the open-source software FreeFem++ [20]. Computer codes are available from the authors upon reasonable request.*

1 R. Fleury, D. L. Sounas, C. F. Sieck, M. R. Haberman, and A. Alú, Sound isolation and giant linear nonreciprocity in a compact acoustic circulator, Science **343**, 516 (2014).
2 Z. Yang, F. Gao, X. Shi, X. Lin, Z. Gao, Y. Chong, and B. Zhang, Topological acoustics, Phys. Rev. Lett. **114**, 114301 (2015), arXiv: 1411.7100.
3 X. Zhang, M. Xiao, Y. Cheng, M. H. Lu, and J. Christensen, Topological sound, Commun. Phys. **1**, 97 (2018), arXiv: 1807.09544.
4 P. Gao, and J. Christensen, Topological vortices for sound and light, Nat. Nanotechnol. **16**, 487 (2021).
5 N. Laforge, R. Wiltshaw, R. V. Craster, V. Laude, J. A. Iglesias Martínez, G. Dupont, S. Guenneau, M. Kadic, and M. P. Makwana, Acoustic topological circuitry in square and rectangular phononic crystals, Phys. Rev. Appl. **15**, 054056 (2021), arXiv: 2012.08014.
6 K. Zhang, F. Hong, J. Luo, and Z. Deng, Topological edge state analysis of hexagonal phononic crystals, Acta Mech. Sin. **38**, 421455 (2022).
7 B. Xia, Z. Jiang, L. Tong, S. Zheng, and X. Man, Topological bound states in elastic phononic plates induced by disclinations, Acta Mech. Sin. **38**, 521459 (2022).
8 M. Z. Hasan, and C. L. Kane, Colloquium: Topological insulators, Rev. Mod. Phys. **82**, 3045 (2010), arXiv: 1002.3895.
9 G. Ma, M. Xiao, and C. T. Chan, Topological phases in acoustic and mechanical systems, Nat. Rev. Phys. **1**, 281 (2019).
10 E. Prodan, and C. Prodan, Topological phonon modes and their role in dynamic instability of microtubules, Phys. Rev. Lett. **103**, 248101 (2009), arXiv: 0909.3492.
11 L. H. Wu, and X. Hu, Scheme for achieving a topological photonic crystal by using dielectric material, Phys. Rev. Lett. **114**, 223901 (2015).
12 C. He, X. Ni, H. Ge, X. C. Sun, Y. B. Chen, M. H. Lu, X. P. Liu, and Y. F. Chen, Acoustic topological insulator and robust one-way sound transport, Nat. Phys. **12**, 1124 (2016), arXiv: 1512.03273.
13 J. Lu, C. Qiu, L. Ye, X. Fan, M. Ke, F. Zhang, and Z. Liu, Observation of topological valley transport of sound in sonic crystals, Nat. Phys. **13**, 369 (2017), arXiv: 1709.05920.
14 M. Miniaci, R. K. Pal, B. Morvan, and M. Ruzzene, Experimental observation of topologically protected helical edge modes in patterned elastic plates, Phys. Rev. X **8**, 031074 (2018), arXiv: 1710.11556.
15 M. Yan, J. Lu, F. Li, W. Deng, X. Huang, J. Ma, and Z. Liu, On-chip valley topological materials for elastic wave manipulation, Nat. Mater. **17**, 993 (2018).
16 J. A. Iglesias Martínez, N. Laforge, M. Kadic, and V. Laude, Topological waves guided by a glide-reflection symmetric crystal interface, Phys. Rev. B **106**, 064304 (2022), arXiv: 2203.02692.
17 J. Zak, Berry's phase for energy bands in solids, Phys. Rev. Lett. **62**,

2747 (1989).
18 P. Delplace, D. Ullmo, and G. Montambaux, Zak phase and the existence of edge states in graphene, Phys. Rev. B **84**, 195452 (2011), arXiv: 1109.4608.
19 Y. F. Wang, T. T. Wang, J. W. Liang, Y. S. Wang, and V. Laude, Channeled spectrum in the transmission of phononic crystal waveguides, J. Sound Vib. **437**, 410 (2018).
20 F. Hecht, New development in freefem++, J. Numer. Math. **20**, (2012).

滑动反射对称声子晶体界面: 主题变化

Vincent Laude, Julio Andrés Iglesias Martínez, Nicolas Laforge, Muamer Kadic, Emil Prodan

摘要 节点可以在晶体界面处使用滑动反射对称性人工合成. 这一特性首次在半晶格常数滑行第一个布里渊区(波数$k = \pm\pi/a$, a表示晶格常数)的X点方形晶格声子晶体中得到证明. 在这里, 考虑四分之一晶格常数滑动反射对称性, 节点可以移动到Γ点($k = 0$). 应用沿x轴连续分级的过程进一步表明条带结构基本不受影响. 特别是拓扑界面波存活在滑动反射对称性仅在分级界面周围局部有效的情况下. 总之, 滑移位错会影响到几排晶格距离, 以恢复为明显的周期性晶体.